POLITECNICO DI TORINO
Repository ISTITUZIONALE

CAROTIDNet: A Novel Carotid Symptomatic/Asymptomatic Plaque Detection System Using CNN-Based Tangent Optimization Algorithm in B-Mode Ultrasound Images

Terms of use:

Publisher copyright

(Article begins on next page)

29 June 2024

RESEARCH ARTICLE

CAROTIDNet: A Novel Carotid Symptomatic/Asymptomatic Plaque Detection System Using CNN-Based Tangent Optimization Algorithm in B-Mode Ultrasound Images

TANWEER ALI [1], **(Senior Member, IEEE), SAMEENA PATHAN** [2], **MASSIMO SALVI** [3],
KRISTEN M. MEIBURGER [3], **(Member, IEEE), FILIPPO MOLINARI** [3], **(Senior Member, IEEE),**
AND U. RAJENDRA ACHARYA [4,5]

[1] Department of Electronics and Communication Engineering, Manipal Institute of Technology, Manipal Academy of Higher Education, Manipal 576104, India
[2] Department of Information and Communication Technology, Manipal Institute of Technology, Manipal Academy of Higher Education, Manipal 576104, India
[3] Biolab, PolitoBIOMed Laboratory, Department of Electronics and Telecommunications, Politecnico di Torino, 10129 Turin, Italy
[4] School of Mathematics, Physics and Computing, University of Southern Queensland, Springfield, QLD 4300, Australia
[5] Centre for Health Research, University of Southern Queensland, Springfield, QLD 4300, Australia

Corresponding author: Sameena Pathan (sameena.bp@manipal.edu)

ABSTRACT Deep learning methods have shown promise for automated medical image analysis tasks. However, class imbalance is a common challenge that can negatively impact model performance, especially for tasks with minority classes that are clinically significant. This study aims to address this challenge through a novel hyperparameter optimization technique for training convolutional neural networks on imbalanced data. We developed a custom Convolutional Neural Network (CNN) architecture and introduced a Tangent Optimization Algorithm (TOA) based on the trigonometric properties of the tangent function. The TOA optimizes hyperparameters during training without requiring data preprocessing or augmentation steps. We applied our approach to classifying B-mode ultrasound carotid artery plaque images as symptomatic or asymptomatic using a dataset with significant class imbalance. On k-fold cross-validation, our method achieved an average accuracy of 98.82%, a sensitivity of 99.41%, and a specificity of 95.74%. The proposed optimization technique provides a computationally efficient and interpretable solution for training deep learning models on unbalanced medical image datasets.

INDEX TERMS Plaque classification, deep learning, carotid artery imaging, tangent optimization algorithm, ultrasound imaging.

I. INTRODUCTION

Atherosclerosis, the buildup of plaque in the arteries, is a major risk factor for cardiovascular diseases such as heart attacks and strokes, which are leading causes of death and disability worldwide. The formation and progression of atherosclerotic plaques significantly impact cardiovascular health and are associated with various disease conditions. According to the World Health Organization, cardiovascular diseases cause over 17 million deaths annually, with over 75% of these deaths occurring in low- and middle-income countries [1].

A key contributor to atherosclerosis is the progressive accumulation of lipid and fibrous elements within the inner layer of the arterial walls – the plaque. Over time, this plaque buildup narrows the lumen of arteries, reducing blood flow to organs and tissues. If left unchecked, it can lead to complete blockage and critical ischemia. While atherosclerosis often develops silently over decades, sudden plaque rupture can trigger life-threatening events such as myocardial infarction or ischemic stroke. Early detection and prevention of plaque formation is therefore crucial to reducing cardiovascular disease risk and mortality rates on a global scale.

The associate editor coordinating the review of this manuscript and approving it for publication was Wojciech Sałabun.

TABLE 1. State of art methods employed for the automated detection of plaque using ultrasound images.

Reference	Method	Image type	Number of images	Performance
Suri et al., 2011 [7]	Texture analysis and SVM classifier	CCA	365	Accuracy: 82.4%; Sensitivity: 82.9%; Specificity: 82.1%
Biswas et al., 2020 [9]	Deep neural network	CCA	250	Accuracy: 89%
Gago et al. 2022 [10]	CNN designed using Bayesian optimization	CCA	4727	Accuracy: 97%, Sensitivity: 0.88; Specificity: 0.97
Molinari et al., 2018 [15]	Bidimensional empirical mode decomposition and entropy features	CCA	1773	Accuracy: 91.43%; Sensitivity: 97.26%; Specificity: 83.22%
Acharya et al., 2013 [20]	Discrete wavelet transform and SVM classifier	CCA	146	Accuracy: 91.7%; Sensitivity: 97%; Specificity: 80%
Afonso et al., 2015 [21]	Mixed features and binary decision rule	CCA	146	Accuracy: 83.5%; Sensitivity: 84.1%; Specificity: 83.7%
Saba et al, 2021. [22]	Transfer learning system for classification	CCA	520	Accuracy: 94.55%
Skandha et al., 2022 [23]	Hybrid deep neural network	CCA	506	AUC: 0.997
Singh et al., 2023 [24]	GoogleNet	CCA	190	Accuracy; 98.20%
Our study	Fully convolutional networks and tangent optimization algorithm	CCA	1773	Accuracy: 98.82%; Sensitivity: 99.41%; Specificity: 95.74%

Characterizing the composition and morphology of atherosclerotic plaques can provide valuable insight into disease pathogenesis and prognosis. Features such as plaque size, lipid content, calcification, ulceration, and neovascularization have all been associated with plaque vulnerability and risk of clinical events. Studying plaque characteristics aids in determining which are more prone to rupture. It also helps in the development of diagnostic techniques, therapies and clinical guidelines for risk stratification and treatment. Non-invasive carotid plaque imaging modalities such as ultrasound, CT and MRI have enabled detailed in vivo plaque analysis [2], leading to a better understanding of disease progression and more effective management approaches, as shown in Fig. 1. Ultrasound imaging is considered one of the most preferred methods for analyzing the morphological aspects of atherosclerotic plaque [3], [4], and can be chosen over CT and MRI as it is real-time, does not use ionizing radiation, and is inexpensive, while still allowing a morphological analysis of changes including ulceration, heterogeneity, and echogenicity in plaques [5]. However, processing ultrasound images is challenging due to poor resolution [6], the presence of manual markers and artifacts.

In recent years, conventional machine learning and deep learning-based techniques have been proposed to characterize symptomatic and asymptomatic plaque, specifically in longitudinal B-mode ultrasound images of the carotid artery [5], [7], [8], [9], [10]. To be specific, radiomic features have been analyzed by developing complex image processing algorithms [8]. Additionally, some researchers have also used segmentation methods to improve the accuracy of classification. Table 1 provides an overview of the related works on plaque classification in longitudinal B-mode ultrasound images of the common carotid artery (CCA). The CCA is
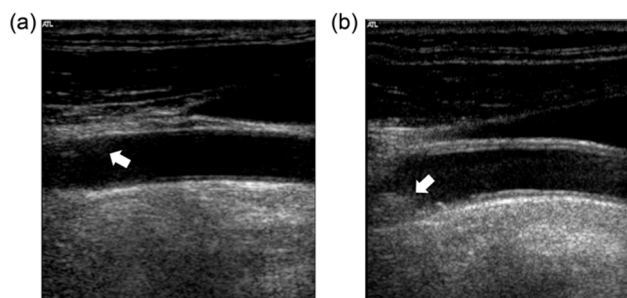
FIGURE 1. Depiction of plaque images, contrasting asymptomatic (a) and symptomatic (b) cases. White arrow indicates the plaque.

typically analyzed to measure the intima-media thickness (IMT) on the far wall of the artery, as an increased IMT value is often considered a precursor to the development of a plaque [11], [12]. Previous studies in the literature have also aimed to classify plaques as either vulnerable and stable by analyzing plaque echogenicity after contrast agent injection [13], [14]. While this method may permit a more in-depth analysis of plaque tissue characterization, it has the drawback of being minimally invasive as it requires the injection of microbubbles into the bloodstream. It is important to note that the dataset used in our study is the same as that used in [15] and represents the largest available collection of carotid plaque image data to date.

One major challenge in plaque classification is the imbalanced nature of the dataset, due to which there is a significant gap in sensitivity and specificity, results in most of the classification tasks [16], [17]. Most researchers employ data balancing techniques such as data augmentation, generating synthetic samples, etc. However, such data balancing techniques increase the computational complexity. In addition,

conventional data augmentation techniques often generate images that are very similar to each other, which can limit their effectiveness in improving model performance [18]. In contrast, images generated by AI systems may not guarantee the preservation of pathological features on synthetic images, which can affect their usefulness in certain applications [19].

The goal of this study is to develop an automated method, called CAROTIDNet, for classifying carotid plaque images into symptomatic versus asymptomatic categories based on morphological characteristics that are extracted from B-mode ultrasound images without the use of any contrast agent. Such a technique could assist physicians in evaluating plaque stability and tailoring medical management accordingly. It may also help identify patients who would benefit most from interventions like endarterectomy.

The proposed method aims to overcome issues associated with classifying unbalanced medical image datasets by employing a novel optimization methodology for identifying optimal convolutional neural network (CNN) hyperparameters. A major contribution of the proposed classification approach is that it eliminates the need for data preprocessing steps to remove artifacts. It can also efficiently handle imbalanced datasets, producing promising accuracy for classifying normal (asymptomatic plaque) and risk (symptomatic plaque) images while avoiding the computational complexity of data augmentation techniques. Plaques were classified as symptomatic or asymptomatic based on whether the patient exhibited symptoms such as transient ischemic attack or stroke. However, it is important to note that asymptomatic does not necessarily mean the plaque is stable or without risk of rupture. Vulnerable plaques can still cause clinical events even in the absence of symptoms. Similarly, stable plaques may remain asymptomatic but still increase the risk of future cardiovascular disease. The proposed method aims to assist physicians in evaluating plaque stability and identify patients who could benefit from medical intervention, regardless of current symptom status. The key contributions are three-fold:

1. A new optimization algorithm based on _trigonometric_ properties of the tangent function is proposed to optimize hyperparameters for classification with an unbalanced plaque image dataset.
2. A CNN architecture, named CAROTIDNet, is developed and its hyperparameters are optimized using a sine-cosine optimization algorithm.
3. The dataset used in this study consists of 1773 images, which is one of the largest available carotid plaque image datasets, allowing for more robust deep learning model development and effective hyperparameter optimization to improve performance.

To the best of our knowledge, this is the first approach that eliminates the need for data augmentation while efficiently handling class imbalance, achieving balanced sensitivity and specificity for classification. The paper is organized as follows: Section II describes the detailed methodology of the proposed tangent optimization algorithm; Sections III and IV

report and discuss the experimental results; Section V concludes with implications drawn from the study.

II. MATERIALS AND METHODS
A. DATASET
The dataset consisted of longitudinal ultrasound images of the carotid arteries in the common tract acquired on 420 patients. All images were from subjects with atherosclerosis that were either in an early stage or showed clearly visible plaques. A total of 1353 images were from symptomatic subjects who exhibited at least one of the following symptoms: amaurosis, transient ischemic attack (TIA), minor stroke, or transient aphasia. An additional 420 images were from asymptomatic subjects. At the time of image acquisition, none of the subjects had experienced a major stroke or had other cerebrovascular diseases.

All images were acquired using an ATL HDI5000 ultrasound scanner equipped with a linear probe operating within a frequency range of 7-12 MHz. Fig. 1 illustrates representative asymptomatic and symptomatic images from the acquired dataset. The images were not subjected to any kind of image pre-processing methods, and none were excluded from the study.

B. HYPERPARAMETER OPTIMIZATION USING PROPOSED METHOD AND CLASSIFICATION
Convolutional neural networks (CNNs) extend the capabilities of traditional neural networks by including additional convolutional and activation functions. The main advantage of CNNs is the incorporation of convolutional filters, which aid in detecting patterns in the data that may not be discernible to the human eye, thus enabling more accurate classification. The overall architecture of the CAROTIDNet is shown in Fig. 2. The convolution and fully connected layers are composed of biases and weights that are trained using optimization algorithms such as Adam, gradient descent, and stochastic gradient descent.

The performance of the CNN is mainly controlled by hyperparameters such as the initial learning rate, momentum, L2 regularization, and number of epochs. The choice of hyperparameters depends heavily on the application. However, tuning hyperparameters is essential for each application to achieve a balanced sensitivity and specificity, especially when dealing with imbalanced medical datasets.

Table 2 provides details of the CNN architecture, including the types and sizes of filters, numbers of filters, and stride values at each layer. Convolution layers are followed by batch normalization, activation functions, and max pooling layers. The network ends with fully connected and softmax classification layers. The batch normalization (BN) layer normalizes the gradients and activation functions. The max pooling layer (MPL) reduces the dimensions of the feature maps and passes them to subsequent convolutional layers. The rectified linear unit (ReLU) performs non-linear mapping, while the final fully connected layer performs classification,
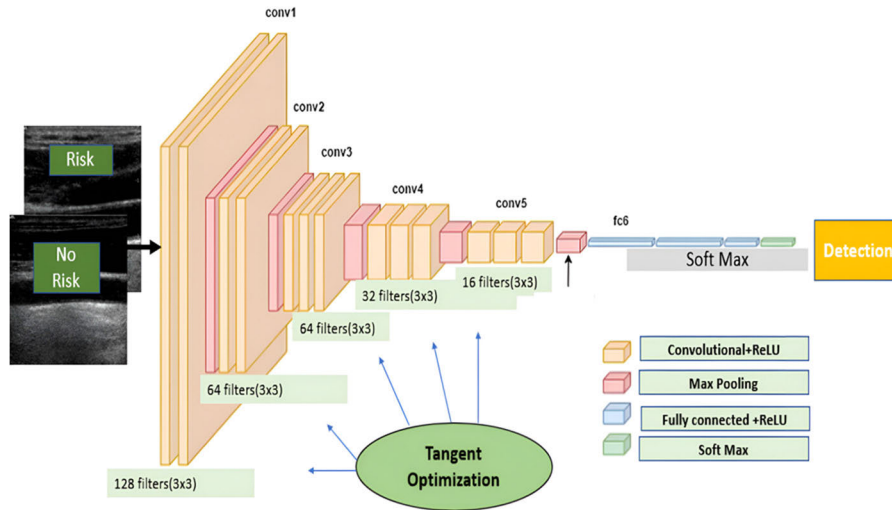
FIGURE 2. Overview of the proposed CNN architecture and optimizing hyperparameters.

TABLE 2. Details of the proposed CNN architecture developed.

Layer	Type	Filter size	Number of filters	Stride
Conv_1	CL+BN+ReLu	3x3	128	1x1
MPL_1		2x2		2x2
Conv_2	CL+BN+ReLu	3x3	64	1x1
MPL_2		2x2		2x2
Conv_3	CL+BN+ReLu	3x3	32	1x1
MPL_3		2x2		2x2
Conv_4	CL+BN+ReLu	3x3	26	1x1
MPL_4		2x2		2x2
Conv_5	CL+BN+ReLu	3x3	8	1x1
MPL_5		2x2		2x2
Conv_6	CL+BN+ReLu	3x3	8	1x1
MPL_6		2x2		2x2
Fully connected layer + Classification Layer			Softmax	

followed by the softmax layer to convert probabilities to numerical outputs. The hyperparameters used in the stochastic gradient descent algorithm for optimization are the learning rate, momentum, L2 regularization, and number of epochs. The learning rate primarily controls the speed of gradient descent by regulating how quickly the neural network learns the problem. The momentum parameter is responsible for accumulating the moving average of gradients in an exponentially decaying manner. L2 regularization, also known as weight decay, causes weights to decay towards zero over time [25], [26], [27]. The number of epochs refers to the number of full passes through the training dataset during optimization. An optimal epoch size is necessary for accurate training of the CNN model, as one epoch is equivalent to the size of the training dataset.

C. OPTIMIZATION USING SINE COSINE ALGORITHM (SCA)
One of the most popular metaheuristic population-based optimization algorithms proposed by Mirjalili [28] is the sine-cosine algorithm (SCA). The optimization initialization

begins with a population group of random solutions. The random solution population set is continuously evaluated based on the objective function. As described in Eq. (1), the SCA consists of exploration and exploitation phases.

$$X_i^{t+1} = X_i^t + r_1 \cdot sin\,(r_2)\,\left|r_3 P_i^t - X_i^t\right| \qquad (1)$$

The exploration phase aids in the location of the area. Further, the exploitation phase reduces the fluctuations that occur by the random solutions as given in Eq. (2).

$$X_i^{t+1} = X_i^t + r_1 \cdot cos\,(r_2)\,\left|r_3 P_i^t - X_i^t\right| \qquad (2)$$

Here t indicates the current iteration number, and i indicates the ith solution at the corresponding X position; P_i indicates the point of destination. The direction of movement between the solution and the destination is guided by the parameter r_1 as given in Eq (3).

$$r_1 = 2 - t\left(\frac{2}{T}\right) \qquad (3)$$

The movement of the particles towards or away from the destination and defining the distance movement using random weights is given by r_2 and r_3.

$$r_2 = 2\pi \cdot rand\,(value) \qquad (4)$$

$$r_3 = 2 \cdot rand\,(value) \qquad (5)$$

If $r_3 > 1$, an emphasizing effect occurs, while if $r_3 < 1$, a deemphasizing effect occurs in the movement towards the optimal solution. The switching between the exploration and exploitation phases is performed by r_4. Exploration takes place if the value of r_4 is less than 0.5, while exploitation occurs if the value is greater than 0.5. Fig. 3 illustrates the convergence curve for the SCA algorithm, considering the upper and lower bound values of the dataset used for tuning the hyperparameters. This convergence curve demonstrates how the objective function value changes as the algorithm optimizes the hyperparameters within the defined bounds.
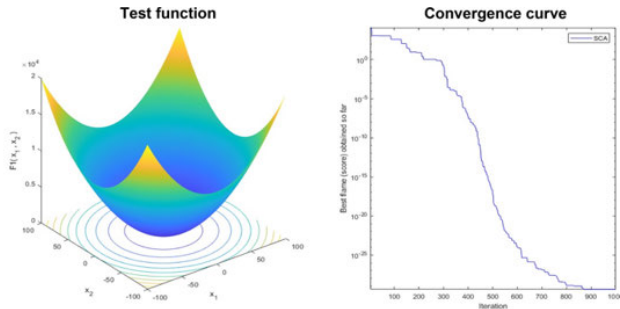
FIGURE 3. Illustration of convergence curve considering the objective function for SCA.

D. TANGENT OPTIMIZATION ALGORITHM (TOA)

The proposed tangent optimization algorithm consists of four sequential phases: (i) Initialization, (ii) Definition of the objective function, (iii) Exploration & exploitation, and (v) Stopping criteria.

1) INITIALIZATION

The goal of the initialization phase is to generate the defined search space for exploration and exploitation.

Rather than random solutions, lower and upper bound values are determined based on the minimum and maximum possible values for each hyperparameter. The search space is represented as a matrix of dimensions NXd, where $N = 50$ (solutions) and $d = 4$ (columns) since four hyperparameters are optimized. This results in a search space of 50x4. The choice between the exploration and exploitation phases is controlled by a mathematical normalization function (NF) calculated from the search space, as shown in Eq. (6)-(7). The NF provides a threshold based on the current iteration and maximum iterations for determining whether exploration or exploitation will be performed during optimization within the defined search space.

$$Criteria = \begin{bmatrix} \textbf{\textit{Exploration, if }} r_1 > NF \\ \textbf{\textit{Exploitation, if }} r_1 \leq NF \end{bmatrix} \quad (6)$$

$$NF = \min(X) + t\left(\frac{\max(X) - \min(X)}{T}\right) \quad (7)$$

where t and T indicate the current and maximum number of iterations. Since the search space is 50×4, we set the maximum iteration value as 200 (50×4).

2) OBJECTIVE FUNCTION

The goal of the optimization algorithm is to predict the optimal hyperparameter values when training on the dataset. One key aspect of designing an optimization algorithm is selecting an appropriate objective function. The tangent optimization algorithm aims to minimize the classification error between predicted and actual values by considering the hyperparameters obtained during exploration and exploitation phases within the bounds of the defined search space. To select the best value for the validation set, the training data is

further split in an 80:20 ratio. The final value for each hyperparameter is chosen based on the error rate calculated from the held-out 20% of the training data.

The pseudocode for the objective function is provided in Algorithm 1. It outlines the process of defining the lower and upper bounds, training the CNN model using stochastic gradient descent with optimized hyperparameters, and evaluating classification errors on the validation set to identify optimal hyperparameters.

Algorithm 1

---

1 Defining the *Lb, and Ub,* $\forall x \in N_{lb}^{ub}$
2 $CNN(SGD\{M, ILR, Ep, L2\ Regularization\}$

   Using $X_i^{t+1} = X_i^t + r_1 Sin(r_2)\left|r_3 P_i^t - X_i^t\right|$, $X_i^{t+1} = X_i^t + r_1 Cos(r_2)\left|r_3 P_i^t - X_i^t\right|$
3 $\forall x \in \{Hyp\}, 0.8\ (Training\ data)$
   $= testing\ the\ values\ obtained$
   $from\ exploitation\ and\ exploration$
   $phase$
4 *Classification Error*
   $= Actual\ values\ (0.2\ Training\ data)$
   $- Predicted\ values(0.2\ Training\ Data)$
5 *Final Hyp = min {Classification Error}*

---

3) EXPLORATATION AND EXPLOITATION

The exploration phase begins by considering the normalization function in conjunction with random variables r_2 and r_3. These random variables are used to control switching between subsequent phases. The ability to flexibly switch between arithmetic operations aids in achieving optimal values for optimization.

A scaling parameter α is introduced to achieve symmetry between the exploration and exploitation phases. Fig. 4 illustrates the convergence curve considering the objective function for the proposed tangent optimization.
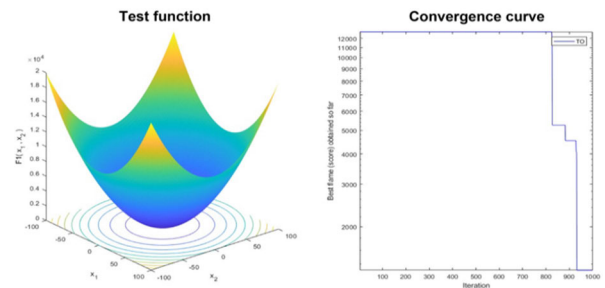

FIGURE 4. Illustration of convergence curve considering the objective function for TOA.

The value of α is calculated as given in Eq. (8). Position update equations incorporating α, the normalization function, random variables and hyperparameters bounds are formulated in Eq. (9)-(10) to govern movement between solutions

during exploration and exploitation.

$$\propto = \frac{t}{T} \qquad (8)$$

$$X_{ij}(t+1)$$
$$= \begin{cases} \frac{X_j}{(\propto + \tan(U\{b\} - L\{b\})\mu + \tan(L\{b\}))} \, if \, r_2 \leq 0.5 \\ X_j \propto \tan(U\{b\} + L\{b\})\mu - \tan(L\{b\})) \, if \, r_2 > 0.5 \end{cases} \qquad (9)$$

$$X_{ij}(t+1)$$
$$= \begin{cases} X_j - \propto \mu \tan(U\{b\} - L\{b\}) + \tan(L\{b\})) \, if \, r_3 \leq 0.5 \\ X_j + \propto \mu \tan(U\{b\} - L\{b\}) - \tan(L\{b\})) \, if \, r_3 > 0.5 \end{cases} \qquad (10)$$

The primary motivation for using the tangent trigonometric function was to address the lead-lag behavior exhibited by sine and cosine functions. Additionally, combining tangent with sine and cosine results in asymmetry of the generated harmonics. This asymmetry could lead to delayed convergence and increased computational complexity in reaching optimal values. Therefore, the tangent function is employed individually for the exploration and exploitation phases, rather than in combination with other trigonometric functions. The exploration phase equations also serve as the initialization function.

During optimization, if the value of r_2 is less than 0.5, the division operator is used in the equations. Conversely, if the value of r_2 is greater than 0.5, the multiplication operator is used. Similarly, the arithmetic operators (+/-) are switched based on whether the value of r_3 is less than or greater than 0.5. This switching technique helps balance the exploration of the search space.

4) STOPPING CRITERIA
The exploration and exploitation phases terminate once the optimal solution is found. The stopping criteria are reaching the maximum number of iterations, as defined by the size of the search space. The search space consists of $50 \times 4 = 200$ possible combinations of hyperparameters since it is represented as a 50×4 matrix. Therefore, the maximum number of iterations is set to 200 to allow full exploration of this defined search space. The exploration and exploitation phases systematically examine the entire space.

III. RESULTS
A. TRAINING PROCESS
The proposed methodology was implemented in MATLAB 2020a on a 64-bit operating system. The entire image dataset consisted of 420 patients, with an average of 10 images acquired per patient. The dataset was initially divided on a patient-wise basis into a training set comprising 80% of the patients and a validation set comprising the remaining 20% of patients. This ensured that images from the same patient did not fall into different sets. A k-fold cross-validation (k =5) was used to evaluate the model.

Algorithm 2

1 *Initialization*: Choose $N = 50$, $d = 4$, search space $= 50 \times 4$, $\min(X)$, $Max(X)$, ; $t = \{1, 2, \dots \dots N\}$ $Lb = \{0.00001, 0.1, 5, 0.001\}$ $Ub = \{0.1, 0.9, 15, 0.1\}$

2 *While $t < T \to$ Compute Nf using* (7), $\propto = \frac{t}{T}$
  if Nf < 0.5, Check for r_2
  if $r_2 \leq 0.5$
    $X_{ij}(t+1) = \frac{X_j}{(\propto + \tan(U\{b\} - L\{b\})\mu + \tan(L\{b\}))}$
  else
    $X_j \propto \tan(U\{b\} + L\{b\})\mu - \tan(L\{b\}))$
  if $r_3 \leq 0.5$
    $X_{ij}(t+1) = X_j - \propto \mu \tan(U\{b\} - L\{b\}) + \tan(L\{b\}))$
  else
    $X_{ij}(t+1) = X_j + \propto \mu \tan(U\{b\} - L\{b\}) - \tan(L\{b\}))$

3 *Create CNN layers $\to 6(CL + ReLu + MPL)$*

4 *Formulate the objective function* : *classification error*
5 *Hyperparameters*
  $= optimal \{SGDM, ILR, Ep, L2 \, Regularization\}$
6 *Best Parameters* : $0.2(training \, data)$

7 *Stopping Criteria* :
  While $t < T_{max}$
    Check $x = best(min(Classification \, error(0.2 \, (train))$
  else
    $t = t + 1$

As the dataset contained images of varying sizes, all images were resized uniformly to $256 \times 256 \times 1$ pixels to retain consistency. The optimized CNN architecture consisted of 5 convolutional layers for classifying images into two categories. Stochastic gradient descent hyperparameters were optimized using two algorithms: SCA and TOA. Fig. 5 illustrates the training progress plots obtained using SCA and TOA. The figure shows that when optimizing an unbalanced dataset with SCA, the performance decreases compared to optimization with the Tangent algorithm, in terms of both classification performance and loss function value.
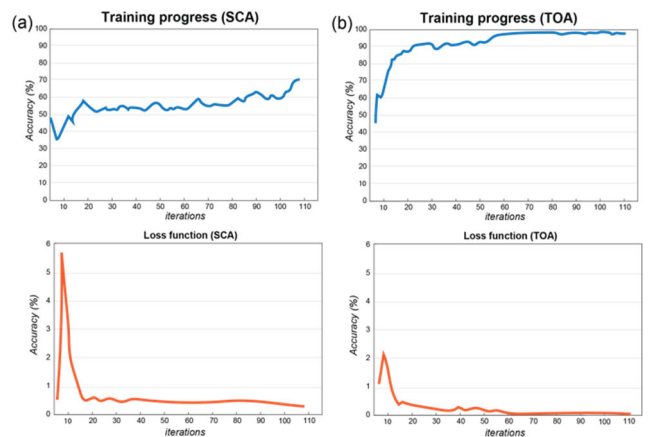

FIGURE 5. Training Progress using CNN model optimized using (a) SCA, and (b) TOA.

B. K-FOLD CROSS-VALIDATION
The proposed classification methodology was evaluated using 5-fold cross-validation on the development set.

Within each fold, the CNN hyperparameters were optimized using TOA. Key metrics including accuracy, sensitivity, specificity, and precision were used to assess CNN performance. Accuracy provides the average correct prediction rate across both classes. Sensitivity indicates the true positive rate for the risk class. Specificity is the true negative rate for the normal class. Precision is the percentage of true positives among the total predicted positives.

Table 3 reports the performance of the CNN model optimized for each fold. The results demonstrate the high performance of our optimized CNN model across all folds. The average accuracy achieved was 98.82%, indicating a high level of correct predictions for both the risk and normal classes. The sensitivity values ranged from 98.53% to 100%, indicating the ability of our model to accurately detect the symptomatic plaque. Moreover, the precision values ranged from 98.53% to 100%, highlighting the high percentage of true positives among the predicted positives.

TABLE 3. Quantitative metrics obtained using k-fold cross-validation for the CNN trained using the TOA.

Fold	Accuracy	Sensitivity	Specificity	Precision
#1	99.38%	100%	96.08%	99.27%
#2	99.07%	99.63%	96.08%	99.27%
#3	99.38%	99.26%	100%	100%
#4	98.76%	99.63%	94.51%	99.27%
#5	97.52%	98.53%	92.16%	98.53%
Average	*98.82%*	*99.41%*	*95.74%*	*99.26%*

C. GRAD-CAM AND EXPLAINABILITY

GRAD-CAM (Gradient-weighted Class Activation Mapping) is a popular method in the field of Explainable Artificial Intelligence (XAI) that provides insights into the decision-making process of deep learning models. By visualizing the areas of an input image that contribute most strongly to the model's prediction, GRAD-CAM helps to interpret and understand the reasoning behind the model's classification.

In Fig. 6, we present grayscale images and their corresponding GRAD-CAM outputs for three different cases. The first two cases represent asymptomatic patients, where the GRAD-CAM of CAROTIDNet shows a focus on the entire lumen. This indicates that the model correctly focuses on the entire length of the vessel wall in these cases.

In contrast, in the symptomatic patient image (case #3), the intensity of the GRAD-CAM is higher near the plaque region. This suggests that CAROTIDNet is able to localize and prioritize the areas associated with plaque, providing valuable information for diagnosing symptomatic plaque. The application of GRAD-CAM as an XAI method enhances the interpretability of CAROTIDNet's predictions, enabling clinicians to gain insights into the model's decision-making process and validating its focus on relevant regions of interest in the images.
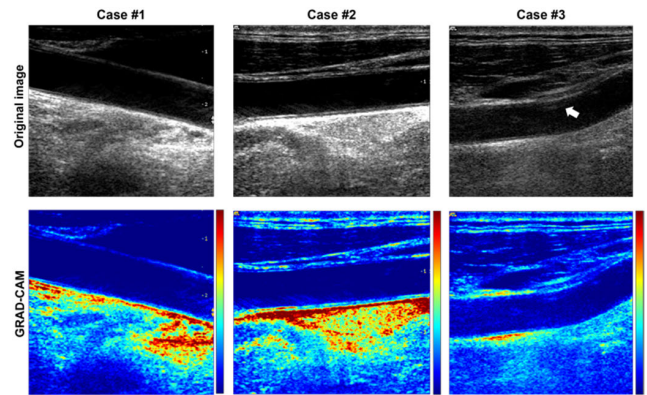
FIGURE 6. Illustration of Grad-CAM for the CAROTIDNet model trained with TOA for three cases. Top row: grayscale ultrasound images of carotid artery plaque. Bottom row: corresponding Grad-CAM heatmaps, highlighting the important regions focused by the model for each prediction.
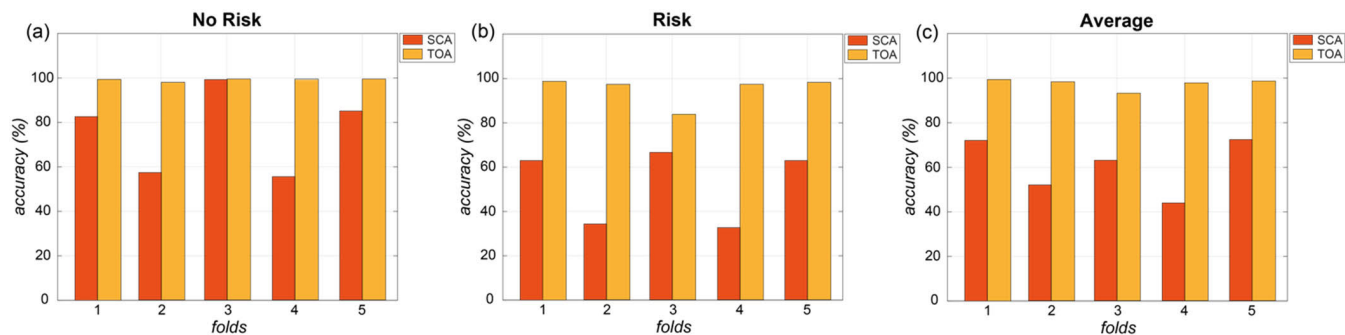
D. ABLATION STUDY

To study the effectiveness of the proposed method, an ablation study is conducted by considering the dataset given in [30]. Since, the dataset consists of 80 images belonging to only risk category, we have concatenated the non risk images from our dataset to the images obtained from [30]. Additionally, since we are proving the robustness of the proposed algorithm considering imbalance in the data, we have 160 images of non-risk category (our dataset) and 80 risk images from external dataset. The initial study termed as first iteration involved testing of the SCA algorithm in the formulated dataset considering the CNN architecture described in Table 2. The study was performed for five folds. The training results obtained for the first iteration are as shown in Fig. The second iteration consisted of testing the proposed optimization algorithm using the CNN architecture described in Table 2. The training results obtained for the second iteration are shown in Fig.

For both iterations, the number of accurately classified risk and non-risk cases is depicted in Fig. As it can be observed, the proposed CAROTIDNet performs better in contrast to the initial SCA optimization algorithm on a dataset consisting of images from two different sources, thereby proving the generalization and robustness of the methodology proposed.

IV. DISCUSSION

Plaque classification plays a crucial role in the detection and management of atherosclerosis, a major risk factor for cardiovascular diseases. Accurate classification of plaques as symptomatic or asymptomatic can assist physicians in tailoring medical management accordingly [1]. In this paper, we have addressed the challenge of unbalanced datasets in plaque classification and proposed an efficient and reliable technique called the Tangent Optimization Algorithm (TOA). Our approach, based on the trigonometric properties of the tangent function, ensures balanced sensitivity and specificity for plaque classification.

FIGURE 7. Performance analysis for the ablation study (a) Accuracy for non risk cases, (b) Accuracy for risk cases, (c) Average accuracy for risk and non risk cases.

The presence of imbalanced datasets poses a significant problem in medical image classification tasks, as it can result in imbalanced sensitivity and specificity outcomes. Traditional data balancing techniques, such as data augmentation, often increase computational complexity and may generate similar images, limiting their effectiveness [18]. In contrast, the TOA algorithm optimizes the hyperparameters of a CNN without the need for data preprocessing steps or data augmentation.

We evaluated the performance of our proposed method and compared it with the state-of-the-art technique, the Sine-Cosine Algorithm (SCA). Our results demonstrate that the TOA algorithm outperforms SCA in terms of accuracy, sensitivity, and specificity. The TOA algorithm achieves balanced performance on both symptomatic and asymptomatic plaque images, effectively addressing the challenge of imbalanced datasets. This indicates the potential of the TOA algorithm to improve the accuracy of plaque classification and assist in identifying patients who require medical interventions.

The advantages of our proposed approach extend beyond improved performance. Our method reduces the computational complexity associated with data preparation by eliminating the need for data preprocessing steps and data augmentation. Additionally, the TOA algorithm provides a reliable and interpretable solution by optimizing hyperparameters based on the trigonometric properties of the tangent function. This ensures that the resulting CNN model captures important features for plaque classification.

Incorporating GRAD-CAM into our analysis further enhances the interpretability of CAROTIDNet's predictions. GRAD-CAM generates heatmaps that highlight the regions of interest in the images, allowing clinicians to visualize the areas that contribute most strongly to the model's decision-making process. This additional information helps in understanding the specific visual features that influence the classification of carotid plaque images. By integrating GRAD-CAM, we strengthen the transparency of CAROTIDNet and provide clinicians with valuable insights into the model's reasoning.

While our study presents promising results, there are several areas for future research in plaque classification.

Firstly, it is important to conduct further investigations to explore the robustness and generalizability of the TOA algorithm on larger and more diverse datasets. This will help assess its performance in different clinical scenarios, including cases with rare histological diseases that may exhibit imbalanced datasets [29]. Few studies have evaluated the performance of DL methods for plaque tissue classification [31], [32], [33]. For instance, in [31], the diagnostic odds ratio was used as a performance evaluation parameter. In [33], radiomic features of the carotid artery were proven to have great potential in predicting new ipsilateral ischemic lesions. Evaluating the algorithm's applicability on various imaging modalities, such as CT and MRI, can provide valuable insights into its effectiveness in different clinical settings. Secondly, the TOA algorithm can be combined with other techniques, such as transfer learning, to further enhance the classification performance

V. CONCLUSION

In this study, we have developed a novel optimization methodology for classifying longitudinal B-mode ultrasound carotid plaque images. Our approach addresses several challenges associated with processing ultrasound images, such as poor resolution, the presence of artifacts, and imbalanced datasets. The proposed methodology incorporates a customized CNN architecture optimized using a sine-cosine optimization algorithm. Additionally, we introduce a novel tangent optimization algorithm that effectively handles the imbalanced nature of plaque image datasets. Unlike traditional data augmentation techniques, our approach does not compromise computational efficiency. The experimental results demonstrate the effectiveness of our approach in classifying symptomatic and asymptomatic plaque images. By achieving balanced sensitivity and specificity, our CNN model shows promise in assisting physicians in evaluating plaque stability and tailoring medical management accordingly. Moreover, eliminating data preprocessing steps for artifact removal further streamlines the classification process. The future work will include evaluating the proposed methodology using Leave One Subject Out (LOSO) cross-validation to better assess the generalization capabilities of the approach. Finally, developing a unified system involving

the segmentation of plaque regions followed by classification could provide a more comprehensive analysis. Segmenting the plaque areas before feeding them to the classification model may help focus the localization and improve prediction accuracy. Integrating segmentation with the current detection framework is an important future direction.

REFERENCES

[1] *Multiple Cause of Death Data on CDC WONDER*. Accessed: Feb. 24, 2024. [Online]. Available: https://wonder.cdc.gov/mcd.html

[2] T. S. Hatsukami, M. S. Ferguson, K. W. Beach, D. Gordon, P. Detmer, D. Burns, C. Alpers, and D. E. Strandness, "Carotid plaque morphology and clinical events," *Stroke*, vol. 28, no. 1, pp. 95–100, Jan. 1997, doi: 10.1161/01.str.28.1.95.

[3] A. Fedak, R. Chrzan, O. Chukwu, and A. Urbanik, "Ultrasound methods of imaging atherosclerotic plaque in carotid arteries: Examinations using contrast agents," *J. Ultrasonogr.*, vol. 20, no. 82, pp. 191–200, Sep. 2020, doi: 10.15557/jou.2020.0032.

[4] A. Fedak, K. Ciuk, and A. Urbanik, "Ultrasonography of vulnerable atherosclerotic plaque in the carotid arteries: B-mode imaging," *J. Ultrasonogr.*, vol. 20, no. 81, pp. e135–e145, Jun. 2020, doi: 10.15557/jou.2020.0022.

[5] M. Biswas, V. Kuppili, T. Araki, D. R. Edla, E. C. Godia, L. Saba, H. S. Suri, T. Omerzu, J. R. Laird, N. N. Khanna, A. Nicolaides, and J. S. Suri, "Deep learning strategy for accurate carotid intima-media thickness measurement: An ultrasound study on Japanese diabetic cohort," *Comput. Biol. Med.*, vol. 98, pp. 100–117, Jul. 2018, doi: 10.1016/j.compbiomed.2018.05.014.

[6] K. Meiburger, M. Salvi, M. Giacchino, U. Acharya, M. Minetto, C. Caresio, and F. Molinari, "Quantitative analysis of patellar tendon abnormality in asymptomatic professional 'Pallapugno' players: A texture-based ultrasound approach," *Appl. Sci.*, vol. 8, no. 5, p. 660, Apr. 2018, doi: 10.3390/app8050660.

[7] R. U. Acharya, O. Faust, A. P. C. Alvin, S. V. Sree, F. Molinari, L. Saba, A. Nicolaides, and J. S. Suri, "Symptomatic vs. asymptomatic plaque classification in carotid ultrasound," *J. Med. Syst.*, vol. 36, no. 3, pp. 1861–1871, Jun. 2012, doi: 10.1007/s10916-010-9645-2.

[8] C. Qian and X. Yang, "An integrated method for atherosclerotic carotid plaque segmentation in ultrasound image," *Comput. Methods Programs Biomed.*, vol. 153, pp. 19–32, Jan. 2018, doi: 10.1016/j.cmpb.2017.10.002.

[9] M. Biswas, L. Saba, S. Chakrabartty, N. N. Khanna, H. Song, H. S. Suri, P. P. Sfikakis, S. Mavrogeni, K. Viskovic, J. R. Laird, E. Cuadrado-Godia, A. Nicolaides, A. Sharma, V. Viswanathan, A. Protogerou, G. Kitas, G. Pareek, M. Miner, and J. S. Suri, "Two-stage artificial intelligence model for jointly measurement of atherosclerotic wall thickness and plaque burden in carotid ultrasound: A screening tool for cardiovascular/stroke risk assessment," *Comput. Biol. Med.*, vol. 123, Aug. 2020, Art. no. 103847, doi: 10.1016/j.compbiomed.2020.103847.

[10] L. Gago, M. D. M. Vila, M. Grau, B. Remeseiro, and L. Igual, "An end-to-end framework for intima media measurement and atherosclerotic plaque detection in the carotid artery," *Comput. Methods Programs Biomed.*, vol. 223, Aug. 2022, Art. no. 106954, doi: 10.1016/j.cmpb.2022.106954.

[11] K. M. Meiburger et al., "Carotid ultrasound boundary study (CUBS): An open multicenter analysis of computerized intima–media thickness measurement systems and their clinical impact," *Ultrasound Med. Biol.*, vol. 47, no. 8, pp. 2442–2455, Aug. 2021, doi: 10.1016/j.ultrasmedbio.2021.03.022.

[12] K. M. Meiburger et al., "Carotid ultrasound boundary study (CUBS): Technical considerations on an open multi-center analysis of computerized measurement systems for intima-media thickness measurement on common carotid artery longitudinal B-mode ultrasound scans," *Comput. Biol. Med.*, vol. 144, May 2022, Art. no. 105333, doi: 10.1016/j.compbiomed.2022.105333.

[13] F. Molinari, W. Liboni, P. Giustetto, E. Pavanelli, A. Marsico, and J. S. Suri, "Carotid plaque characterization with contrast-enhanced ultrasound imaging and its histological validation," *J. Vascular Ultrasound*, vol. 34, no. 4, pp. 175–184, Dec. 2010, doi: 10.1177/154431671003400402.

[14] V. Rafailidis, X. Li, P. S. Sidhu, S. Partovi, and D. Staub, "Contrast imaging ultrasound for the detection and characterization of carotid vulnerable plaque," *Cardiovascular Diagnosis Therapy*, vol. 10, no. 4, pp. 965–981, Aug. 2020, doi: 10.21037/cdt.2020.01.08.

[15] F. Molinari, U. Raghavendra, A. Gudigar, K. M. Meiburger, and U. R. Acharya, "An efficient data mining framework for the characterization of symptomatic and asymptomatic carotid plaque using bidimensional empirical mode decomposition technique," *Med. Biol. Eng. Comput.*, vol. 56, no. 9, pp. 1579–1593, Sep. 2018, doi: 10.1007/s11517-018-1792-5.

[16] F. Marzola, K. M. Meiburger, and M. Salvi, "Innovative temporal loss function for segmentation of fine structures in ultrasound images," in *Proc. IEEE Int. Ultrason. Symp. (IUS)*. Montreal, QC, Canada: IEEE, Sep. 2023, pp. 1–4, doi: 10.1109/ius51837.2023.10308305.

[17] F. Marzola, K. M. Meiburger, F. Molinari, and M. Salvi, "Exploring the impact of learning paradigms on network generalization: A multi-center IMT study," in *Proc. 24th Int. Conf. Digit. Signal Process. (DSP)*, Jun. 2023, pp. 1–5, doi: 10.1109/DSP58604.2023.10167892.

[18] E. D. Cubuk, B. Zoph, D. Mané, V. Vasudevan, and Q. V. Le, "AutoAugment: Learning augmentation strategies from data," in *Proc. IEEE/CVF Conf. Comput. Vis. Pattern Recognit. (CVPR)*. Long Beach, CA, USA: IEEE, Jun. 2019, pp. 113–123, doi: 10.1109/CVPR.2019.00020.

[19] M. Salvi, F. Branciforti, F. Molinari, and K. M. Meiburger, "Generative models for color normalization in digital pathology and dermatology: Advancing the learning paradigm," *Expert Syst. Appl.*, vol. 245, Jul. 2024, Art. no. 123105, doi: 10.1016/j.eswa.2023.123105.

[20] U. R. Acharya, O. Faust, A. P. C. Alvin, G. Krishnamurthi, J. C. R. Seabra, J. Sanches, and J. S. Suri, "Understanding symptomatology of atherosclerotic plaque by image-based tissue characterization," *Comput. Methods Programs Biomed.*, vol. 110, no. 1, pp. 66–75, Apr. 2013, doi: 10.1016/j.cmpb.2012.09.008.

[21] D. Afonso, J. Seabra, L. M. Pedro, J. F. E. Fernandes, and J. M. Sanches, "An ultrasonographic risk score for detecting symptomatic carotid atherosclerotic plaques," *IEEE J. Biomed. Health Informat.*, vol. 19, no. 4, pp. 1505–1513, Jul. 2015, doi: 10.1109/JBHI.2014.2359236.

[22] L. Saba, S. S. Sanagala, S. K. Gupta, V. K. Koppula, J. R. Laird, V. Viswanathan, M. J. Sanches, G. D. Kitas, A. M. Johri, N. Sharma, A. Nicolaides, and J. S. Suri, "A multicenter study on carotid ultrasound plaque tissue characterization and classification using six deep artificial intelligence models: A stroke application," *IEEE Trans. Instrum. Meas.*, vol. 70, pp. 1–12, 2021, doi: 10.1109/TIM.2021.3052577.

[23] S. S. Skandha, A. Nicolaides, S. K. Gupta, V. K. Koppula, L. Saba, A. M. Johri, M. S. Kalra, and J. S. Suri, "A hybrid deep learning paradigm for carotid plaque tissue characterization and its validation in multi-center cohorts using a supercomputer framework," *Comput. Biol. Med.*, vol. 141, Feb. 2022, Art. no. 105131, doi: 10.1016/j.compbiomed.2021.105131.

[24] S. Singh, P. K. Jain, N. Sharma, M. Pohit, and S. Roy, "Atherosclerotic plaque classification in carotid ultrasound images using machine learning and explainable deep learning," *Intell. Med.*, vol. 2023, Jul. 2023, Art. no. S2667102623000414, doi: 10.1016/j.imed.2023.05.003.

[25] C. Cortes, M. Mohri, and A. Rostamizadeh, "L_2 regularization for learning kernels," 2012, *arXiv:1205.2653*.

[26] T. van Laarhoven, "L2 regularization versus batch and weight normalization," 2017, *arXiv:1706.05350*.

[27] F. C. Soon, H. Y. Khaw, J. H. Chuah, and J. Kanesan, "Hyper-parameters optimisation of deep CNN architecture for vehicle logo recognition," *IET Intell. Transp. Syst.*, vol. 12, no. 8, pp. 939–946, Oct. 2018, doi: 10.1049/iet-its.2018.5127.

[28] S. Mirjalili, "SCA: A sine cosine algorithm for solving optimization problems," *Knowl.-Based Syst.*, vol. 96, pp. 120–133, Mar. 2016, doi: 10.1016/j.knosys.2015.12.022.

[29] M. Salvi, N. Michielli, K. M. Meiburger, C. Cattelino, B. Cotrufo, M. Giacosa, C. Giovanzana, and F. Molinari, "Cyto-Knet: An instance segmentation approach for multiple myeloma plasma cells using conditional kernels," *Int. J. Imag. Syst. Technol.*, vol. 34, no. 1, pp. 1–14, Jan. 2024, doi: 10.1002/ima.22984.

[30] C. P. Loizou, C. S. Pattichis, M. Pantziaris, and A. Nicolaides, "An integrated system for the segmentation of atherosclerotic carotid plaque," *IEEE Trans. Inf. Technol. Biomed.*, vol. 11, no. 6, pp. 661–667, Nov. 2007.

[31] S. S. Skandha et al., "3-D optimized classification and characterization artificial intelligence paradigm for cardiovascular/stroke risk stratification using carotid ultrasound-based delineated plaque: Atheromatic™ 2.0," *Comput. Biol. Med.*, vol. 125, Oct. 2020, Art. no. 103958.

[32] S. Assi, M. Jayabalan, V. Parakh, J. Assi, A. A. Hamid, and D. A.-J. Obe, "Predicting incidence of stroke via supervised machine learning methods on class imbalanced data," in *Non-Invasive Health Systems Based on Advanced Biomedical Signal and Image Processing*. Boca Raton, FL, USA: CRC Press, 2024, pp. 128–144.

[33] R. Zhang, Q. Zhang, A. Ji, P. Lv, J. Acosta-Cabronero, C. Fu, J. Ding, D. Guo, Z. Teng, and J. Lin, "Prediction of new cerebral ischemic lesion after carotid artery stenting: A high-resolution vessel wall MRI-based radiomics analysis," *Eur. Radiol.*, vol. 33, no. 6, pp. 4115–4126, Dec. 2022.

MASSIMO SALVI is currently an Assistant Professor with Politecnico di Torino. In addition to his work in biomedical signal and image processing, he is also actively engaged in the field of artificial intelligence and deep learning. He has experience in the development of hybrid techniques that combine AI-based methods and mathematical-statistical techniques to address complex problems in biomedical research. His research is primarily focused on the development of automated solutions for fluorescence and optical microscopy, with a particular emphasis on the analysis and interpretation of cellular and tissue images.

KRISTEN M. MEIBURGER (Member, IEEE) is mainly active in the field of biomedical image processing, with a focus on vascular network analysis using biomedical optical imaging methods (i.e., optical coherence tomography angiography and photoacoustics) and radiomics and deep learning applications. She is also active in the field of biomedical signal processing and particularly, in ultrasound image beamforming methods.
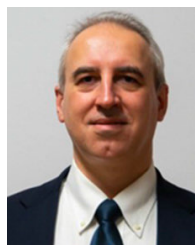
FILIPPO MOLINARI (Senior Member, IEEE) is a Full Professor with Politecnico di Torino, where he leads research in several areas of biomedical engineering. His primary research interests include biomedical signal processing, image processing, and ultrasound technology, with a focus on developing advanced diagnostic tools for a range of medical applications. In addition to his work in these areas, his research activities also include the non-invasive characterization of tumor vascularization, neuroimaging for the advanced assessment of neurodegenerative disorders, and neurovascular and metabolic assessment of cerebral autoregulation.

TANWEER ALI (Senior Member, IEEE) is currently an Associate Professor with the Department of Electronics and Communication Engineering, Manipal Institute of Technology, Manipal Academy of Higher Education, Manipal. He is an active researcher in the field of microstrip antennas, wireless communication, and microwave imaging. He has been listed in top 2% scientists across the world, in 2021 and 2022, by the prestigious list published by Stanford University, USA, indexed by Scopus. He has published more than 130 papers in reputed web of science (SCI) and Scopus-indexed journals and conferences. He has seven Indian patents, of which three have published. He is on the Board of a Reviewers of journals, such as IEEE TRANSACTIONS ON ANTENNAS AND PROPAGATION, IEEE ANTENNAS AND WIRELESS PROPAGATION LETTERS, IEEE ACCESS, *IET Microwaves, Antennas and Propagation*, *Electronics Letter* (IET), *Wireless Personal Communications* (Springer), *International Journal of Electronics and Communications* (AEU), *Microwave and Optical Technology Letters* (Wiley), *International Journal of Antennas and Propagation* (Hindawi), *Advanced Electromagnetics*, *Progress in Electromagnetics Research* (PIER), *KSII Transactions on Engineering Science*, *International Journal of Microwave and Wireless Technologies*, *Frequenz*, *Radioengineering*, and IEEE OPEN JOURNAL OF ANTENNAS AND PROPAGATION, with an emphasis on the analysis and interpretation of cellular and tissue images.

U. RAJENDRA ACHARYA received the Ph.D., D.Eng., and D.Sc. degrees. He is a Professor of artificial intelligence in healthcare with the School of Mathematics, Physics, and Computing, University of Southern Queensland, Australia; a Distinguished Professor with the International Research Organization for Advanced Science and Technology, Kumamoto University, Japan; and an Adjunct Professor with the University of Malaya, Malaysia. His funded research has accrued cumulative grants exceeding six million Singapore dollars. He has authored over 800 publications, including 750 in refereed international journals, 42 in international conference proceedings, and 17 books. He has received over 80 000 citations on Google Scholar (with an H-index of 141). According to the Essential Science Indicators of Thomson, he has been ranked in the top 1% of the highly cited researchers for the last seven consecutive years (2016–2022) in computer science. His research interests include biomedical imaging and signal processing, data mining, visualization, and the applications of biophysics for better healthcare design and delivery. He is on the editorial boards of many journals and has served as a guest editor for several AI-related issues.

SAMEENA PATHAN is currently an Assistant Professor with the Department of Information and Communication Technology, Manipal Institute of Technology, Manipal Academy of Higher Education, Manipal. Her research interests include pattern recognition, medical image analysis, artificial intelligence, and machine learning.

• • •